Pergamon

Tetrahedron Vol. 51, No. 9, pp. 2593-2604, 1995

0040-4020/95 $9.50+0.00

0040-4020(95)00008-9

Conformational Study of Dolastatin 10

Témin Alattia†, Florence Roux#, Joël Poncet#*, Adrien Cavé†, and Patrick Jouin#

#Laboratoire des Mécanismes Moléculaires des Communications Cellulaires (UPR 9023 CNRS),
Centre CNRS-INSERM, rue de la Cardonille, 34094 Montpellier Cedex 5, France

†Centre de Biochimie Structurale (UMR 9955 CNRS, U 414 INSERM), Faculté de Pharmacie,
15, Avenue Charles-Flahaut, 34060 Montpellier Cedex, France

Abstract: The potent antineoplasic pseudopeptide dolastatin 10 isolated from the sea hare *Dolabella auricularia* was examined by a combination of one and two dimensional NMR techniques (DQF-COSY, HOHAHA, ROESY, HMQC, and HMBC) followed by restrained molecular-dynamics (MD) simulations to elucidate its conformation in solution (DMSO). The study showed that dolastatin 10 exists in two different conformations corresponding to a *cis-trans* isomerisation of the Dil-Dap amide bond.

INTRODUCTION

Dolastatins are a family of antineoplastic pseudopeptides isolated from the Indian Ocean sea hare, *Dolabella auricularia*.[1] Among them, dolastatin 10 shows the most potent activity (IC_{50} = 0.05 nM and 0.4 nM on murine P388 and L1210 lymphocytic leukemia cells, respectively).[2] This compound binds to the β

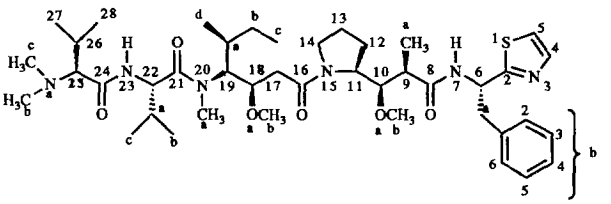

Dolavaline (*Dov*) Valine (*Val*) Dolaisoleuine (*Dil*) Dolaproine (*Dap*) Dolaphenine (*Doe*)

subunit of tubulin and inhibits its polymerisation (IC_{50} = 1.2 μM).[3] However, there is no good correlation between this latter property and its cytotoxicity.[4] Some routes for synthesizing this compound have been already described.[5] In connection with our interest in biologically active peptides of marine origin,[6] we recently developed an efficient stereoselective synthesis.[7] We now wish to report the results of a conformational study of dolastatin 10 (in DMSO solution) by NMR spectroscopy and molecular-dynamics (MD) simulations.

RESULTS AND DISCUSSION

NMR studies

^1H and ^{13}C NMR spectra of synthetic dolastatin 10 dissolved in DMSO-d6 were recorded at 305 K. Under these conditions, both types of spectra presented evidence for an equilibrium between two distinct species slowly interconverting on the NMR time scale and corresponding to a 60:40 ratio. This situation is also observed in CD_2Cl_2 or CD_3OD where two species are observed[2]

Resonance assignment. A complete study was performed by 2D ^1H spectroscopy. Protons resonances were assigned by careful analysis of the DQF-COSY[8], HOHAHA[9] and ROESY[10] spectra. Most of the ^{13}C resonances including carbonyl groups and quaternary carbons could be assigned by heteronuclear spectroscopy on the basis of the previously assigned proton resonances. The HMQC[11] and HMBC[12] spectra were recorded on the same sample under similar experimental conditions. The ^1H and ^{13}C chemical shifts are reported in Table 1.

Table 1. ^1H and ^{13}C Chemical Shifts Values of Dolastatin 10 (DMSO-d6, 305 K)

Atoms	δ (^1H) [ppm]		δ (^{13}C) [ppm]	
(n°)	Major conformation	Minor conformation	Major conformation	Minor conformation
2			172.58	
4	7.79	7.77	119.72	
5	7.65	7.62	119.72	
6	5.52	5.39	50.38	51.33
6a	3.50	3.42	39.03	39.21
6a'	3.06	3.97	39.05	39.19
6b1			137.69	
6b2 and 6b6	7.20		128.81	
6b3 and 6b5	7.26		127.91	
6b4	7.16		125.97	
7	8.85	8.62		
8			173.10	172.82
9	2.23	2.19	43.01	
9a	1.10	1.06	14.83	14.60
10	3.33	3.79	84.71	80.88
10b	3.25	3.20	60.03	59.87
11	3.15	3.42	57.78	58.13
12	1.66	1.61	24.82	23.86
12'	1.22	1.31	24.82	23.86
13	1.75	1.77	27.75	23.98
13'	1.42	1.45	27.75	23.98
14	3.56	3.45	45.85	46.84
14'	3.01	3.19	45.85	46.84
16			168.75	168.36
17	2.35	2.42	34.10	36.83

Table 1 (continued)

17'	2.19	2.23	34.10	36.83
18	3.98	3.97	77.14	
18b	3.20	3.16	56.73	56.63
19	4.70	4.61	54.81	55.54
19a	1.79	1.76	28.26	28.67
19b	1.29	1.31	24.99	
19b'	0.89		24.99	
19c	0.76		15.09	
19d	0.87		8.84	
20a	3.07	2.99	30.91	31.24
21			172.57	
22	4.63	4.84	53.50	53.57
22a	2.03	1.96	29.57	
22b	0.97	0.92	18.08	
22c	0.92	0.92	18.56	
23	broad signal 7.85 to 8.19			
24			undetected signal	
25	broad signal 2.65		broad signal 69.70[a]	
25b	broad signal 2.23		38.02	
25c	broad signal 2.23		38.02	
26	1.95		23.40	
27	0.89		19.31	
28	0.74		18.58	

a: ^{13}C chemical shift was determined from a weak signal in the HMQC spectrum reprocessed using the first 256 points of each FID in order to increase the signal -to-noise ratio.

Conformational parameters. ROESY spectra were recorded at different mixing times ranging from 50 to 300 ms and the integrations of the observed cross peaks were used to construct buildup curves. A total of

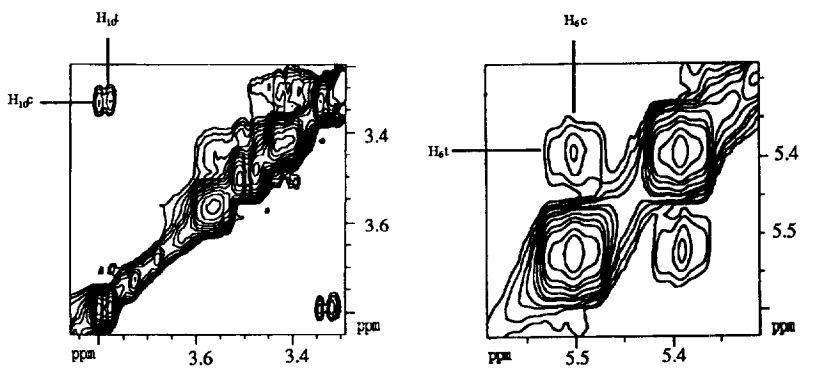

Figure 1. Negative cross-peaks due to chemical exchange H10*cis*/H10 *trans* (left) and H6c/H6t (right) as observed in the ROESY spectrum of dolastatin 10 in DMSO-d6 at 305K and 400 MHz.

217 ROESY peaks were observed for both species. In addition to the positive ROESY cross peaks, some negative correlations were observed characteristic of a chemical exchange between protons belonging to distinct species as for instance protons H-10c/H-10t or H-6c/H-6t shown in Figure 1. This clearly indicates the presence of two structures slowly interconverting on the NMR timescale.

A proline-like residue (Dap) or an N-methyl amide group (Dil) is quite capable of inducing a state of equilibrium between *cis* and *trans* amide bonds. The cross peaks H-11/H-17, H-11/H-17', H-10/H-17, H-10/H-17' involving the Dil /Dap residues observed in the major component suggest a *cis* conformation for the amide bond 15-16. In contrast the cross peaks H-14/H-17 and H-14/H-17', exclusively detected in the minor component, as shown in Figure 2, describe a *trans* amide bond 15-16.

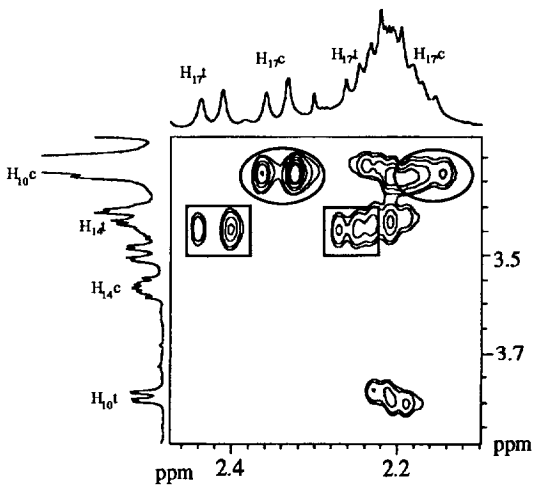

Figure 2. Positive ROE cross-peaks observed between H17/H17' and H14 (□ *trans* conformer) and between H17/H17' and H10 (○ *cis* conformer) as observed in the ROESY spectrum of dolastatin 10 in DMSO-d6 at 305 K and 400 MHz.

The observation of a strong ROE between Me-20a and H-22 for both conformers clearly indicates that the methylated amide bond 20-21 remains *trans* in both cases. It is therefore obvious that the chemical exchange between both species present in solution is due to isomerisation about the 15-16 amide bond. There is no evidence for the presence of *cis* conformation for any of the other amide bonds which are hence considered to be *trans*.

Among the 217 cross peaks observed in the ROESY spectra for both conformers, 82 could be quantified by analysis of buildup curves. Distances were calculated using the cross-peaks of the geminal protons H-6a/H-6a' and H-14/H-14' as reference for both conformers. The average distance separating these protons was assumed to be 1.75 Å. Distance values obtained from the buildup curves reported in Table 2 were used as restraints in structure calculations. Significant differences in some intra-residue and sequential

ROEs were noted between both conformers (underlined values). ROEs of longer range were only observed for the *cis* conformer.

Table 2. Protons Distances Derived from the ROESY Experiment

Residues	Atom numbers		d (H, H) (Å)	
			Cis conformer	*Trans* conformer
Doe	6	6a	w (2.59)	w (3.09)
	6	6a'	s (3.05)	s (2.58)
	6	6b2-6	2.35 (2.40)	2.58 (3.75)
	6	7	2.53 (2.79)	2.79 (2.79)
	6a	6a'	1.75 ref (1.75)	1.75 ref (1.75)
	6a	6b2-6	2.90 (2.82)	2.79 (3.48)
	6a	7	- (3.60)	3.06 (2.63)
	6a'	7	2.43 (2.51)	2.44 (2.39)
	6b2-6	7	3.36 (3.05)	3.19 (5.40)
Dap	10	9	2.26 (3.05)	- (3.00)
	10	9a	2.40 (2.80)	2.40 (3.00)
	10	11	- (2.50)	2.23 (2.48)
	10b	9a	2.62 (3.10)	2.54 (3.95)
	10b	10	2.23 (2.45)	- (2.80)
	10b	12	3.33 (4.10)	- (4.95)
	10b	13	3.50 (3.60)	- (4.10)
	11	9a	- (4.72)	3.55 (4.70)
	11	12'	2.20 (2.28)	2.35 (-)
	13'	14	2.36 (2.38)	2.33 (2.34)
	14	14'	1.75 ref (1.79)	1.75 ref (1.79)
Dil	17	19a	2.16 (3.60)	2.36 (4.21)
	17	19d	2.98 (5.05)	- (3.60)
	17	18	m (2.60)	m (2.51)
	17'	18	w (3.03)	w (3.04)
	20a	17	2.36 (2.30)	- (2.56)
	20a	17'	2.29 (2.25)	- (5.29)
	20a	18	2.86 (3.20)	2.83 (4.20)
	20a	19a	2.15 (2.22)	2.15 (3.85)
	20a	19b	2.87 (2.70)	2.99 (5.20)
	20a	19b'	2.97 (4.20)	2.48 (5.20)
	20a	19c	3.59 (4.20)	3.48 (5.41)
	20a	19d	3.30 (4.48)	2.68 (3.83)
	19	18	2.42 (2.78)	2.83 (2.32)
	19	18b	2.48 (2.31)	3.05 (4.49)
	19	19a	2.96 (2.98)	- (2.65)
	19	19c	2.89 (3.10)	2.96 (3.00)
	19	19d	2.34 (2.55)	- (3.87)
	19d	18b	- (4.15)	2.99 (4.92)

Table 2 (continued)

Val	22	22a	2.56 (2.38)	2.64 (2.47)
	22	22bc	2.36 (2.37)	2.24 (3.10)
Doe-Dap	6b2-6	11	3.15 (3.65)	- (5.80)
	7	9	2.07 (2.22)	- (2.22)
	7	9a	3.24 (4.06)	3.18 (4.23)
	7	10	- (3.63)	3.26 (3.52)
	7	11	3.44 (2.28)	- (2.00)
	7	12'	3.53 (3.06)	3.23 (3.35)
Dap-Dil	9a	18b	- (8.83)	2.77 (5.05)
	10b	18	2.14 (2.45)	2.25 (4.66)
Dil-Val	18b	22a	3.52 (4.15)	- (3.90)
	18b	22b	3.25 (3.80)	m (5.60)
	20a	22	1.88 (2.36)	1.92 (2.67)
	20a	22a	2.98 (3.51)	2.99 (3.45)
	20a	22b	2.85 (3.90)	-
Doe-Val	6	22a	4.55 (4.32)	-
	6	22c	2.98 (3.42)	-
	6b2-6	22c	m (2.32)	-
Doe-Dil	6	20a	2.88 (2.20)	-
	6b2-6	18b	3.02 (3.65)	-
	6b2-6	20a	3.16 (3.00)	-
Dov-Dap	10	27/28	4.85 (5.40)	-

s: strong but non quantifiable ROE; m: medium non quantifiable ROE; w: weak non quantifiable ROE. The underlined values are highly significant.
Values in parenthesis indicate distances after MD simulations. In the cases where pseudoatom correction was used this distance corresponds to the shortest one measured from the different rotamers.

Coupling constants. The ^3J homonuclear coupling constants were mainly measured from a pure absorption double-quantum-filtered COSY (DQF-COSY)[8] and when possible from a 1D ^1H NMR spectrum. The results reported in Table 3 show similar values for both species, within the limits of the accuracy of the measurements. Coupling constants between protons belonging to the backbone characterize ϕ and ψi angles, whereas the side-chain coupling constants involve χi angles (definitions of these angles are given in ref. 13). The backbone contains four amide bonds but only two exhibit an amide proton (Dov-Val and Dap-Doe). Because of the broadened Dov signals, the coupling constants for this residue could not be measured.

Both ϕ angles of Doe and Val residues correspond to large coupling constants (9 Hz), typical of an extended β structure.[14] Due to the methylation of N-20 of Dil and the presence of a proline-like ring in the Dap residue the ψ angles for these residues could not be assessed via coupling constants.

The observed side-chain coupling constants suggested the presence of different rotamers populations. The quite different coupling constants measured for H-6/H-6a (small constant) and for H-6/H-6a' (large constant) in addition to a strong ROE between H-7 and H-6a' and a weak one between H-7 and H-6a indicated the presence of a large excess of the g+ rotamer (74%) with a small amount of t (21%) for $\chi 1$ of dolaphenine.[15] The side chain of the Dil residue shows a strong coupling constant between protons H-19 and H19a ($\chi 1$), thus indicating a large population of rotamer g+. The lower constant observed between H-22 and

H-22a led to a smaller amount of the rotamer g+ (60%). No information is available for the the side chain (χ1) of Dov residue. The extended backbone of Dil and Dap compared to Ile and Pro is spanned by dihedral angles ψ1 and ψ2. The observed values of the coupling constants associated with these angles do not exclude, as in the case of χ1 angles, the presence of a state of conformational equilibrium between the corresponding rotamers.

Table 3. Vicinal Coupling Constants Measured for Dolastatin 10 (DMSO, 305 K)

Residues	atoms numbers	dihedral angles[a]	^{3}J [Hz] *cis*conformation	^{3}J [Hz] *trans*conformation
Doe	7 - 6	ϕ	9	9
	6 - 6a'	χ1	11	11
	6 - 6a	χ1	5	5
Dap	9 - 9a	χ'	6.5	6.5
	9 - 10	ψ2	10	10
	10 - 11	ψ1	4	4
Dil	18 - 17	ψ2	10	10
	18 - 17'	ψ2	4	4
	18 - 19	ψ1	6	6
	19 - 19a	χ1	11	11
Val	22 - 22a	χ1	9	9
	22 - 23	ϕ	9	9

[a]: for the definition of angles, see ref 13

Stereospecific assignment. H-6a and H-6a' could be easily differentiated by their chemical shifts (Table 1) and coupling constants with H-6 (5 Hz and 11Hz, respectively). The large coupling constant (11 Hz) observed for H6-H6a' indicated that these two protons were *trans*. The observation of a strong NOE between H-6 and H-6a, on the one hand, and between H-7 and H-6a', on the other hand, led to the stereospecific assignment of H-6a as Pro*S* and H-6a' as Pro*R*. This assignement is in agreement with Kobayashi's rule which predicts that the Pro*R* proton has the lowest chemical shift.[16]

Structure calculations under available restraints solved the ambiguity of the stereospecific assignment of the 17/17' protons. The remaining prochiral systems were not assigned stereospecifically.

Conformational analysis (MD simulations)

Conformational analyses were performed by simulated annealing in vacuo using 50 and 32 ROE constraints derived from the previous NMR analysis for the *cis* and *trans* conformations, respectively. These were, mainly, intra-residue ROEs (30 for the *cis* conformer and 25 for the *trans* state), versus fewer sequential ROEs (14 and 7, respectively). Longer range ROEs were only observed for the *cis* conformer (6). Differences between distances observed for comparable sets of protons in both conformers varied up to 0.6 Å for the sequential and the intra-residue ROEs. The main variations concerned the Dil residue. Since no medium range ROEs were found for the *trans* conformer, "non-contacts" were introduced in the simulations of this conformation by setting the lower distance bounds of unobserved contacts to the theoretical distance

limit of observation of the Overhauser effect (i.e. 5 Å). Pseudo atom corrections were made for the aromatic rings and whenever stereospecific assignements were absent. Angular constraints were not included in the structure calculations. Some 200 structures were sampled along the 200 ps dynamics run at 900 K and their coordinates stored after cooling to 300 K. The dihedral angles of amide bonds were set to 180° in both conformers by application of a forcing potential, except for the Dil-Dap bond of the *cis* conformer which was set to 0°. Two distinct sets of structures corresponding to the *cis* and the *trans* conformers were generated. Compared to ROESY data, no violation of distances were observed after MD simulations (Table 2).

Dolastatin 10 in its *cis* conformation folds around the central Dil-Dap bond into a compact structure (Figure 3) as witnessed by ROE contacts between protons from opposite ends of the molecule. Comparison

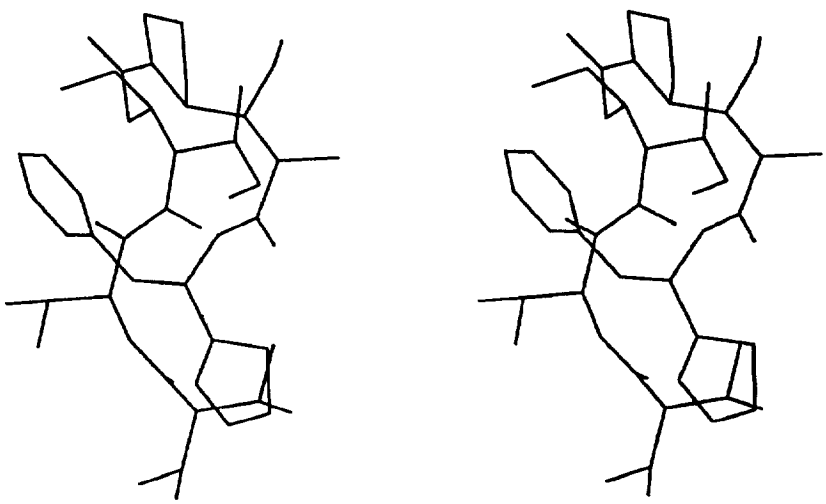

Figure 3. Stereoview of the *cis* conformer of dolastatin 10

of heavy atom coordinates by means of r. m. s., showed good convergence of the calculated *cis* structures for the backbone and side chains. Exception is however made for the N-terminal Dov residue which showed a certain degree of flexibility. This fact can be related to the broadening of the Dov proton signals resulting from slow conformational exchange. Additionally, the thiazole ring, at the other extremity of the molecule, alternated throughout the simulation between two orientations (ψ) separated by an angle of approximatively 120° (Figure 4).

On the other hand, the *trans* conformer exhibited a less compact structure as evidenced by the lack of medium range ROEs. The calculated structures did not converge as well as for the *cis* conformer (Figure 4). Comparison of torsion angles ϕ, ψi, χi and ω for both structures in Figure 5 shows that the *cis-trans* isomerisation at the Dil-Dap amide bond poorly affects both the C-terminal segment (Dap-Doe) and the N-terminal one (Dov-Val). Moreover, the relative ϕ/ψ values for the Val and Doe residues are characteristic of a β structure in both conformers.[14] The Dov residue remains poorly defined in both structures. The main changes concern the Dil residue. While the ψ2 angle remains close to 150° in both conformers, ψ1 and ψ3

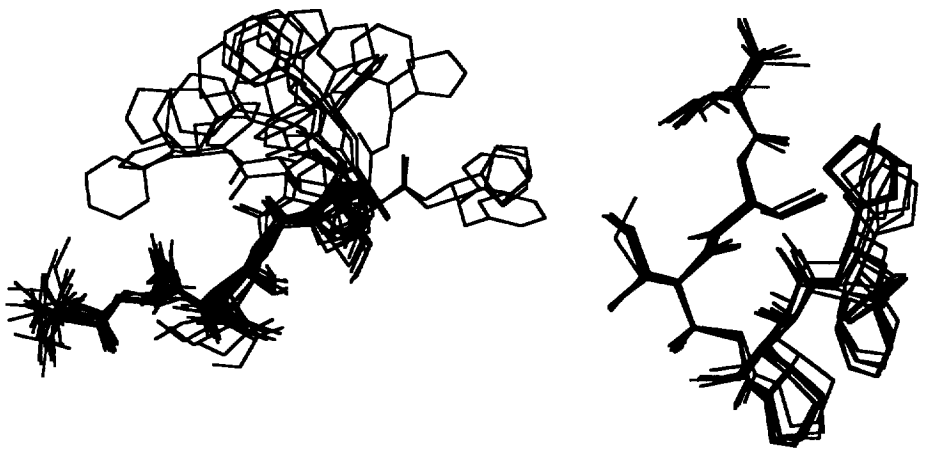

Figure 4. Overlay of structures sampled from the 200 coordinate sets for the trans and cis isomers

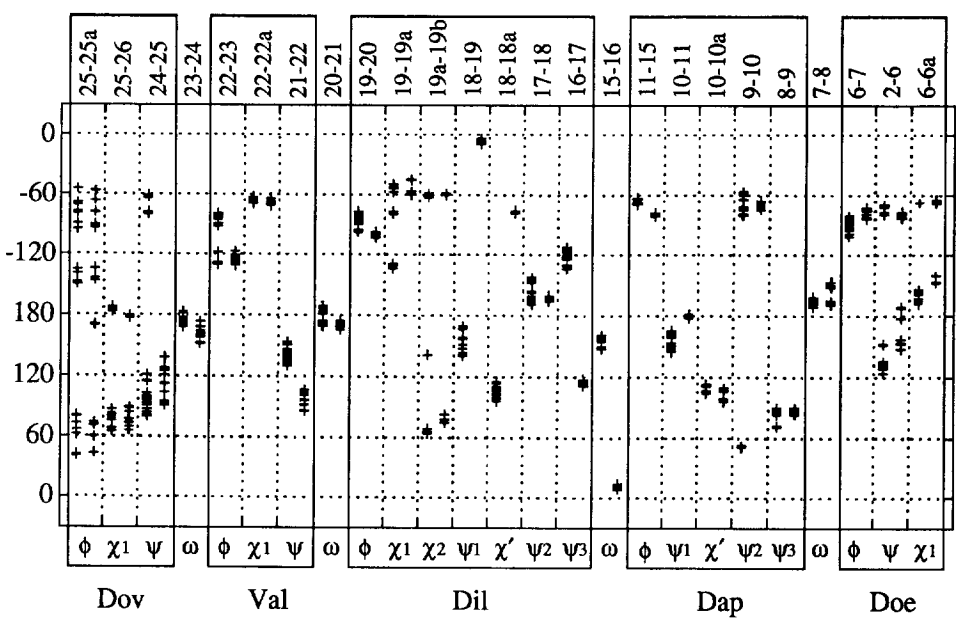

Figure 5. Distribution of the dihedral angles over the 200 calculated structures (left column: *trans* conformer; right column: *cis* conformer)

rotate about 160° and 120°, respectively. The values of the $\psi 1$ angle (160° in the *trans* conformer and 0° in the *cis* conformer) must lead to similar coupling constants for H-18/H-19 in both conformers; this was

confirmed by the experimental data (Table 3). However, in the case of $\psi 3$ there is no experimental data to confirm the calculated angle values. The calculated H-18/H-19 distance is 0.4 Å longer in the *trans* conformation. These changes are probably the consequence of the *cis-trans* isomerisation of the Dil-Dap peptide bond.

The coupling constants together with the ROEs observed between the H-17/H-18 and H-17'/H-18 pairs allow protons H-17 and H-17' to be assigned stereospecifically. The non-equivalence of both coupling constant exclude the presence of the g^- rotamer; on the other hand, the value of $\psi 2$ excludes the g^+ one. The remaining rotamer implies that H-17 is the Pro*R* proton, and H-17' the Pro*S*..

The isomerisation of the Dil-Dap bond leads to the interconversion between an extended structure (*trans*) and a compact one (*cis*) (Calculations on unrestrained structures lead to a difference of 8 kcal/mol in favor of the *cis* conformer and to a barrier to rotation of 28 kcal/mol).This brings us to a possible central role for the C-15/C-16 bond which might act as a hinge in the middle of the molecule. This could have biological significance.[17] At this stage, we should note that the *cis* disposition of the Dil-Dap bond allows hydrophobic interactions to take place between molecular segments surrounding the Dap entity. In a relatively polar solvent like DMSO, the overall stability of the molecule is enhanced in spite of the locally unfavourable *cis* peptide bond. On the other hand, a *trans* peptide bond is energetically more favourable, but implies a deployed structure with few, or no, hydrophobic contacts. In either case, there are antagonist factors acting upon the stability of the molecule with almost the same resulting effect. This can explain the closely populated *cis* and *trans* states of dolastatin 10 in DMSO.

CONCLUSION

This study shows that the dolastatin 10, in solution in DMSO, exhibits two conformational families resulting from a *cis* to *trans* isomerisation of the Dil-Dap peptide bond. We have evoked the probable effect of solvent polarity on the stability of both forms, and the role of the Dil-Dap entity as a conformational switch between a compact *cis* form, and a more stretched *trans* structure. The modelling study shows considerable mobility of the end residues, Dov and Doe. The more internal residues, Val and Dap, are better defined with almost identical sets of rotamers in both *cis* and *trans* structures. In contrast, the *cis*-to-*trans* isomerisation of the C15-C16 amide bond, induces large and well-defined changes of the central Dil residue. Structure-activity relationships studies are now in progress to confirm the biological relevance of this phenomenon.

EXPERIMENTAL PART

NMR spectroscopy

Experiments were carried out on a *Bruker-AMX-400* and a *Bruker-AMX-600* MHz spectrometer. For all experiments, the concentration of synthetic dolastatin 10[7] was 20 mg/ ml in DMSO.

DQF-COSY spectrum [8] (at 305 K, 600 MHz). Phase-sensitive in F_1 using TPPI; 1024 experiments of 4096 data points in F2 were collected with 96 scans per FID; relaxation delay 1s; sweep width 5050 Hz in F_1 and F_2; quadrature detection, single zero filling in both dimensions, apodisation with a shifted sine bell.

HOHAHA spectrum [9] (at 305 K, 400 MHz). Phase-sensitive in F_1 using TPPI; 512 experiments of 2048 data points in F2 were collected with 72 scans per FID; relaxation delay 1s; mixing time 35.7 ms; sweep width 5050 Hz in F_1 and F_2; single zero filling in both dimensions, apodization with a shifted sine bell and base line correction .

ROESY spectrum [10] (at 305 K, 400 MHz). Phase-sensitive in F_1 using TPPI; 512 experiments of 2048 data points in F2 were collected with 80 scans per FID; relaxation delay 1s; mixing times ranged from 50 to 300 ms; sweep width 5050 Hz in F_1 and F_2; quadrature detection, single zero filling in both dimensions, apodization with a shifted sine bell and base line correction. .

HMQC spectrum [11] (at 305 K, 400 MHz). Phase-sensitive in F_1 using TPPI; 1024 experiments of 2048 data points in F2 were collected with 64 scans per FID; relaxation delay 0.4 s; refocusing delay 3 ms; sweep widths 5050 and 19000 Hz in the ^1H and ^{13}C dimension, respectively; quadrature detection, single zero filling in both dimensions, apodisation with a shifted sine bell.

HMBC spectrum [12] (at 305 K, 400 MHz) using a low-pass filter to suppress one bond $^1J_{C-H}$; 1024 experiments of 2048 data points in F2 were collected with 192 scans per FID; relaxation delay 0.3 s; refocusing delay 50 ms; sweep widths 5050 and 23315 Hz in the ^1H and ^{13}C dimension respectively.

Molecular Dynamics simulations

The simulations were performed with the *DISCOVER* software package (version 2.1) using the *CVFF* force field *(Biosym Technologies)* on *Silicon Graphics-4D/30* work station. The starting molecules (the *cis* and *trans* conformers) were manually built with the *INSIGHT II (Biosym)* molecular graphics program and energy minimised. The MD simulations were carried out in vacuo. The simulations started with the experimental distance restraints (lower distances were set to 2 Å and the upper ones to the values listed in Table 2 after pseudoatom corrections). The distance restraints were applied using a force constant of 15 kcal $mol^{-1}.Å^{-2}$. These restrained structures were energy-minimised at 300 K by the steepest descent method for 0.1 ps followed by a conjugate gradient for 1 ps until the root mean square of the gradients was 10^{-3} kcal $Å^{-1}$. A simulated annealing procedure was then applied: the temperature was raised to 900 K by steps of 300 K, and the dynamics were allowed to run for 200 ps. Coordinate sets of structures were sampled every 1 ps and cooled to 300 K. These were then minimised by the procedure described above.

Energy barrier calculations

The 200 coordinate sets generated by the *cis* conformer calculations were submitted to a non restrained energy minimisation, followed by a 1 ps run of dynamics at 300 k and a final minimisation step.The Dil-Dap ω angle was then forced from 0° to 180° with steps of 18° by applying a forcing potential and energy minimisation. A plot of total energy against rotation angle was then established for each one of the 200 structures. A rough estimate of the barrier to rotation is given by the difference between the maximum energy ($\omega = 90°$) and the energy of the unconstrained *cis*-isomer.

Acknowledgements

This research was supported by funds from the Association pour la Recherche sur le Cancer. We are grateful to Dr. S. L. Salhi for help in revising this manuscript.

REFERENCES AND NOTES

1. Pettit, G. R.; Kamano, Y.; Herald, C. L.; Fujii, Y.; Kizu, H.; Boyd, M. R.; Boettner, F. E.; Doubek, D.L.; Schmidt, J. M.; Chapuis, J. C. *Tetrahedron* **1993**, *49*, 9151-9170.
2. Pettit, G. R.; Kamano, Y.; Herald, C. L.; Tuinman, A. A.; Boettner, F. E.; Kizu, H.; Schmidt, J. M.; Baczynskyj, L.; Tomer, K. B.; Bontems, R. J. *J. Am . Chem. Soc.* **1987**, *109*, 6883-6885.
3. Bai, R.; Pettit, G. R.; Hamel, E. *J. Biol. Chem.* **1990**, *265*, 17141-17149.
4. Bai, R.; Roach, M. C.; Jayaram, S. K.; Barkoczy, J.; Pettit, G. R.; Luduena, R. F.; Hamel, E. *Biochem. Pharm.* **1993**, *45*, 1503-1515.
5. a) Pettit, G. R.; Singh, S. B.; Hogan, F.; Lloyd, P.; Herald, C. L.; Burkett, D. D.; Clewlow, P. *J. Am. Chem. Soc.* **1989**, *111*, 5463-5465.
   b) Tomioka, K.; Kanai, M.; Koga, K. *Tetrahedron* **1991**, *32* , 2395-2398.
   c) Shiori, T.; Hayashi, K.; Hamada, Y. *Tetrahedron* **1993**, *49*, 1913-1924.
6. a) Jouin, P.; Poncet, J.; Dufour, M. N.; Pantaloni, A.; Castro, B. *J. Org. Chem.* **1989**, *54*, 617-627.
   b) Patino, N.; Frerot, E.; Galeotti, N.; Poncet, J,. Dufour, M. N.; Coste, J.; Jouin, P. *Tetrahedron* **1992**, *48*, 4115-4122.
7. Roux, F.; Maugras, I.; Poncet, J.; Niel, G.; Jouin, P. *Tetrahedron* . **1994**, *18*, 5345-5360.
8. Derome, A.; Williamson, M. *J. Magn. Reson.* **1990**, *88*, 177-185.
9. Bax, A.; Davis, D. G. *J. Magn. Reson.* **1985**, *65*, 355-360.
10. Bax, A.; Davis, D. G. *J. Magn. Reson.* **1985**, *63*, 207-213.
11. Bax, A.; Subramanian, S. *J. Magn. Reson.* **1986**, *67*, 565-569.
12. Bax, A.; Summers, M. F. *J. Am. Chem. Soc.* **1986**, *108*, 2093-2094.
13. Nomenclature of the torsional angles is based on the recommendations of the IUPAC-IUB Commission on Biochemical Nomenclature (*Biochemistry* **1970**,*9*, 3471-3479). Dil and Dap residues present two additional backbone bonds in comparison with α-amino acids; thus, in the case of dolaisoleuine, $\psi 1$ refers to the sequence N-20, C-19, C-18, C-17, $\psi 2$ to the sequence C-19, C-18, C-17, C-16, etc.
14. Ramakrishnan, C.; Ramachandran, G. N. *Biophys. J.* **1965**, *5*, 909-916.
15. Pachler, K. G. P. *Spectrochim. Acta* **1964**, *20*, 581-587.
16. Kobayashi, J.; Higashijima, T.; Miyazawa, T. *Int. J. Pept. Protein Res.* **1984**, *24*, 40-47.
17. a) Pardi, A.; Billeter, M.; Wüthrich, K. *J. Mol. Biol.* **1984**, *180*, 741-745.
    b) Stein R. L. *Adv. Protein Chem.* **1993**, *44*, 1-24.

(*Received in Belgium* 25 *May* 1994; *accepted* 15 *December* 1994)